AIMS Mathematics, 10(2): 2415–2443.
DOI: 10.3934/math.2025113
Received: 17 November 2024
Revised: 06 December 2024
Accepted: 09 December 2024
Published: 11 February 2025

https://www.aimspress.com/journal/Math

Research article

Application of Caputo-Fabrizio derivative in circuit realization

A. M. Alqahtani[1], Shivani Sharma[2,*], Arun Chaudhary[3] and Aditya Sharma[4]

[1] Department of Mathematics, Shaqra University, Riyadh, Saudi Arabia
[2] Department of Mathematics, Amity University Rajasthan, Jaipur, India
[3] Department of Mathematics, Rajdhani College, University of Delhi, Delhi, India
[4] Department of Electronics Science, University of Delhi, Delhi, India

* **Correspondence:** Email: sharmashivani045@gmail.com.

Abstract: This work incorporates a hyperchaotic system with fractional order Caputo-Fabrizio derivative. A comprehensive proof of the existence followed by the uniqueness is detailed and the simulations are performed at distinct fractional orders. Our results are strengthened by bridging a gap between the theoretical problems and real-world applications. For this, we have implemented a 4D fractional order Caputo-Fabrizio hyperchaotic system to circuit equations. The chaotic behaviors obtained through circuit realization are compared with the phase portrait diagrams obtained by simulating the fractional order Caputo-Fabrizio hyperchaotic system. In this work, we establish a foundation for future advancements in circuit integration and the development of complex control systems. Subsequently, we can enhance our comprehension of fractional order hyperchaotic systems by incorporating with practical experiments.

Keywords: fractional derivative; hyperchaotic system; numerical solutions; simulations; nonlinear dynamical systems; circuit realization
Mathematics Subject Classification: 34H10, 34C28, 37M05, 26A33

1. Introduction

In recent years, fractional derivatives [1] have emerged as a valuable tool in the modeling and analysis of complex systems in various scientific and technical disciplines. Unlike traditional integer-order derivatives, fractional derivatives provide a more flexible and accurate framework for representing the memory and hereditary characteristics of diverse processes. The study of fractional derivatives encompasses various definitions tailored to specific contexts and applications. These definitions incorporate noninteger orders, introducing nuanced interpretations crucial for modeling complex phenomena with memory and hereditary properties. From the Riemann-Liouville [1]

definitions to Caputo [1], Caputo-Fabrizio [2], and Atangana-Baleanu [3] definitions, each offers distinct advantages in mathematical rigor, computational feasibility, and compatibility with diverse physical systems. An understanding of these definitions is quite essential for effectively applying fractional calculus across disciplines such as physics [4–6], engineering [7–9], biology [10–12], etc., where they are crucial in enhancing analytical precision and improving modeling efficacy. The theory of fractional derivatives can also be applied to fractals. Fractals [13] are often characterized by self-similarity where parts of a fractal resemble the whole structure at different scales. A fractal derivative [14] generalizes the concept of a derivative to the irregular, non-smooth structures that are common in fractals. In classical calculus, derivative measures the rate of change of a function. However, in fractals, due to irregularities and infinite details, traditional differentiation methods are not directly applicable. A two-scale fractal derivative [15] refers to the generalization of a classical derivative, particularly in the context of fractal geometry, where the concept of smoothness and differentiability becomes more nuanced due to self-similarity and irregularity of fractals. A two-scale fractional derivative analyzes the rate of change over two distinct fractional orders providing insight into the multi-scale nature of the fractal. Applications of two-scale fractal derivatives can be seen in [16, 17].

The Caputo-Fabrizio derivative is a notable extension of the Caputo derivative, enabling a more precise depiction of physical systems that exhibit the memory effect. This derivative has a non-singular kernel, making it ideal for modeling real-world problems that exhibit an exponential decay behavior. Additionally, the Caputo-Fabrizio derivative provides precise solutions to nonlinear differential equations in a shorter amount of time. Its versatility and theoretical robustness continue to contribute significantly to advance our understanding and application [18–20] of fractional calculus in practical settings.

Hyperchaotic systems have undergone significant advancements since its first introduction by Rossler [21]. These include the development of distinct systems such as one proposed by Erkan et al. [22] in two dimensions for image encryption. A hyperchaotic system in 2D was constructed by Zhu et al. [23] which has applications in color image encryption and pseudo-random number generation. Tang et al. [24] gave a 2D chaotic system for secure communications. Further advancements include 3D hyperchaotic systems studied by Li et al. [25] for a secure transmission. In this progression, a system was developed by Zhi et al. [26] through the extension of a 3D autonomous chaotic framework. Sahasrabuddhe and Laiphrakpam [27] studied an application of a 3D hyperchaotic system in multiple-image encryption. Wang et al. [28] coined a dynamics in a 4D hyperchaotic system. Nestor et al. [29] introduced a 4D hyperchaotic system encompassing dynamic analysis, synchronization, and its application. The complex behavior of hyperchaotic systems has been widely used in fields like information processing, electronics, neuroscience, communications, and beyond. These applications include image encryption [30, 31], random number generation [32, 33], secure communication [24, 34, 35], audio encryption [36], and video encryption [37].

Fractional derivatives [1] also unfold a vast array of applications within hyperchaotic systems, offering a dynamic toolkit to explore and harness their intricate dynamics. By incorporating derivatives of fractional order, hyperchaotic systems can model complex behaviors that integer-order models might not capture completely. This incorporation adds further complexity to the dynamics of hyperchaotic systems encompassing, anomalous diffusion, nonlocal interactions, and long-range memory effects.

Yousefpour et al. [38] presented a fractional-order hyperchaotic economic system. Pan et al. [39]

studied the chaos synchronization with two different fractional orders. Shi et al. [40] investigated the dynamics of a fractional-order hyperchaotic system and identified its potential for use in image encryption. The aforementioned systems facilitate the development of advanced control techniques, synchronization strategies [41, 42], and encryption techniques for a broad spectrum of real-world applications including confidential communications [43, 44] and image encoding [45, 46], among others.

The following hyperchaotic system was proposed by Fu et al. [47] in 4D

$$\begin{aligned}
\frac{d\,x}{d\,t} &= a\,(y - x) + u, & x(0) &= x_0,\\
\frac{d\,y}{d\,t} &= c\,y - 10\,x\,z, & y(0) &= y_0,\\
\frac{d\,z}{d\,t} &= -b\,z + 10\,x\,y, & z(0) &= z_0,\\
\frac{d\,u}{d\,t} &= d\,y + x^2, & u(0) &= u_0,
\end{aligned} \tag{1.1}$$

where a, b, c are constants, $d > 0$ is a variable parameter and x, y, z, u are driving variables. This hyperchaotic system posseses stability, chaotic behavior, and many more physical properties. In their work, experimental validation was performed using Matlab, Multisim, and STM32. The outcomes of their experiments consistently corroborate the theoretical basis for employing this hyperchaotic system in hands-on applications. Subsequently, utilizing the keys derived from this system's hyperchaotic generator, audio encoding is implemented on the STM32 integrated hardware system using a cross-XOR mechanism. Their findings demonstrate the feasibility of the audio encoding technique utilizing this hyperchaotic system highlighting its simplicity of implementation, nonlinear properties, and algorithmic complexity. These attributes render it applicable not only to audio encryption but also to image encryption, video encryption, and other related domains.

As the fractional derivatives enhance complexity in the chaotic behavior of a system, in this work, we extend the hyperchaotic system proposed by Fu et al. [47] to a hyperchaotic system of fractional order using the Caputo-Fabrizio derivative. The existence and uniqueness of the solution of this fractional order hyperchaotic system are detailed and simulations are performed for different fractional orders. This study extends beyond theoretical exploration and aims for real-world applications. For this, we have implemented this 4D fractional order Caputo-Fabrizio hyperchaotic system into circuit equations. We use a digital oscilloscope in Mutisim to realize the circuit and Matlab to perform the simulations for the fractional order Caputo-Fabrizio hyperchaotic system. The chaotic behaviors obtained through circuit realization are compared with the phase portrait diagrams obtained by simulating the fractional order hyperchaotic system.

2. Preliminaries

Definition 1. *[2] For an integrable function g on $\mathbb{R}$, the Caputo-Fabrizio derivative of order ε is given as*

$$^{CF}\mathbb{D}_t^{\varepsilon}(g(t)) = \frac{Q(\varepsilon)}{1-\varepsilon}\int_0^t exp\Big(\frac{-\varepsilon(t-s)}{1-\varepsilon}\Big)g'(s)ds, \quad 0 < \varepsilon < 1, \tag{2.1}$$

where $Q(\varepsilon)$ is a normalizing function such that $Q(0) = 1 = Q(1)$.

Definition 2. *[2] Let g be a function which is integrable on $\mathbb{R}$, with $t > 0$, $0 < \varepsilon < 1$, and the Caputo-Fabrizio fractional integral of order ε is:*

$$\mathcal{I}^{\mathcal{CF}\,\varepsilon}_{\ t}\{g(t)\} = \Psi\, g(t) + \vartheta \int_0^t g(s)ds, \quad t > 0, \tag{2.2}$$

where $\Psi = \frac{2\,(1-\varepsilon)}{(2-\varepsilon)\,Q(\varepsilon)}$, $\vartheta = \frac{2\,\varepsilon}{(2-\varepsilon)\,Q(\varepsilon)}$, *and* $Q(0) = Q(1) = 1$.

3. Fractional order hyperchaotic system with Caputo-Fabrizio derivative

In this part, we extend the 4D hyperchaotic system to the fractional order hyperchaotic system by using the Caputo-Fabrizio derivative. The fractional order hyperchaotic system with the Caputo-Fabrizio derivative is as follows:

$$\begin{aligned}
{}^{CF}_{0}\mathbb{D}^{\varepsilon(t)}_{0}\{x(t)\} &= a\,(y - x) + u, & x(0) = x_0,\\
{}^{CF}_{0}\mathbb{D}^{\varepsilon(t)}_{0}\{y(t)\} &= c\,y - 10\,x\,z, & y(0) = y_0,\\
{}^{CF}_{0}\mathbb{D}^{\varepsilon(t)}_{0}\{z(t)\} &= -b\,z + 10\,x\,y, & z(0) = z_0,\\
{}^{CF}_{0}\mathbb{D}^{\varepsilon(t)}_{0}\{u(t)\} &= d\,y + x^2, & u(0) = u_0,
\end{aligned} \tag{3.1}$$

where a, b, c are constants, $d > 0$ is a variable parameter, and *x, y, z, and u* are driving variables.

3.1. Existence & uniqueness

We present a thorough proof establishing the existence of a unique solution for the 4D fractional order Caputo-Fabrizio hyperchaotic system.

Theorem 1. *If for some constans k_1, k_2, k_3, k_4, the functions $V_1(t, x)$, $V_2(t, y)$, $V_3(t, z)$, $V_4(t, u)$ satisfy the condition given below:*

$$\begin{aligned}
&\|V_1(t, x_1) - V_1(t, x_2)\| \le k_1\|x_1(t) - x_2(t)\|,\\
&\|V_2(t, y_1) - V_2(t, y_2)\| \le k_2\|y_1(t) - y_2(t)\|,\\
&\|V_3(t, z_1) - V_3(t, z_2)\| \le k_3\|z_1(t) - z_2(t)\|,\\
&\|V_4(t, u_1) - V_4(t, u_2)\| \le k_4\|u_1(t) - u_2(t)\|,
\end{aligned} \tag{3.2}$$

where

$$\begin{aligned}
V_1(t, x) &= a\,(y - x) + u,\\
V_2(t, y) &= c\,y - 10\,x\,z,\\
V_3(t, z) &= -b\,z + 10\,x\,y,\\
V_4(t, u) &= d\,y + x^2.
\end{aligned} \tag{3.3}$$

The conditions given by Eq (3.2) *are Lipschitz conditions. The above conditions are contractions if* $k_i < 1, i = 1, 2, 3, 4$.

Proof. To begin, we start with V_1. Let x_1, x_2 be two distinct functions.

$$\begin{aligned} &\|V_1(t,x_1) - V_1(t,x_2)\| = \|(a\,y - a\,x_1 + w) - (a\,y - a\,x_2 + w)\| \\ &= \|a(x_1 - x_2)\| \\ &\leq a\,\|x_1 - x_2\|. \end{aligned} \tag{3.4}$$

Let $a = k_1$, and we have $\|V_1(t,x_1) - V_1(t,x_2)\| \leq k_1\,\|x_1 - x_2\|$. This shows the Lipschitz condition holds for $V_1(t,x)$. In addition, if $k_1 < 1$, then it is a contraction.

Next, consider

$$\begin{aligned} &\|V_2(t,y_1) - V_2(t,y_2)\| = \|(c\,y_1 - 10\,x\,z) - (c\,y_2 - 10\,x\,z)\| \\ &= \|c\,y_1 - 10\,x\,z - c\,y_2 + 10\,x\,z\| \\ &\leq c\,\|y_1 - y_2\|. \end{aligned} \tag{3.5}$$

Taking $c = k_2$, we have $\|V_2(t,y_1) - V_2(t,y_2)\| \leq k_2\,\|y_1 - y_2\|$. This proves the Lipschitz condition for $V_2(t,y)$. Also, if $k_2 < 1$, then it is a contraction.

Now, consider

$$\begin{aligned} &\|V_3(t,z_1) - V_3(t,z_2)\| = \|(-b\,z_1 + 10\,x\,y) - (-b\,z_2 + 10\,x\,y)\| \\ &\| - b\,z_1 + 10\,x\,y + b\,z_2 - 10\,x\,y\| \\ &\| - b(z_1 - z_2)\| \\ &\leq b\|z_1 - z_2\|. \end{aligned} \tag{3.6}$$

Taking $b = k_3$, we have $\|V_3(t,z_1) - V_3(t,z_2)\| \leq k_3\,\|z_1 - z_2\|$. This proves the Lipschitz condition for $V_3(t,z)$. Further, if $k_3 < 1$, then it is a contraction.

Also,

$$\|V_4(t,u_1) - V_4(t,u_2)\| \leq k_4\|u_1 - u_2\|. \tag{3.7}$$

This shows that the functions V_1, V_2, V_3, and V_4 satisfy the Lipschitz condition. □

We now demonstrate the existence of the model configurations by applying a fixed-point hypothesis. To achieve this, we employ the method outlined in [48]. Consider the system given by Eq (3.1)

$$\begin{aligned} x(t) - x(0) &= {}_0^{CF}I_t^{\alpha} V_1(t,x), \\ y(t) - y(0) &= {}_0^{CF}I_t^{\alpha} V_2(t,y), \\ z(t) - z(0) &= {}_0^{CF}I_t^{\alpha} V_3(t,z), \\ u(t) - u(0) &= {}_0^{CF}I_t^{\alpha} V_4(t,u). \end{aligned} \tag{3.8}$$

Employing (2.2), the equations given by (3.8) evolve as:

$$\begin{aligned} x(t) &= x(0) + \Psi V_1(t,x) + \vartheta \int_0^t V_1(s,x)ds, \\ y(t) &= y(0) + \Psi V_2(t,y) + \vartheta \int_0^t V_2(s,y)ds, \end{aligned}$$

$$\begin{aligned} z(t) &= z(0) + \Psi V_3(t,z) + \vartheta \int_0^t V_3(s,z)ds, \\ u(t) &= u(0) + \Psi V_4(t,u) + \vartheta \int_0^t V_4(s,u)ds. \end{aligned} \tag{3.9}$$

This is then followed by the presentation of the recursive method:

$$\begin{aligned} x_n(t) &= \Psi V_1(t,x_{n-1}) + \vartheta \int_0^t V_1(s,x_{n-1})ds, \\ y_n(t) &= \Psi V_2(t,y_{n-1}) + \vartheta \int_0^t V_2(s,y_{n-1})ds, \\ z_n(t) &= \Psi V_3(t,z_{n-1}) + \vartheta \int_0^t V_3(s,z_{n-1})ds, \\ u_n(t) &= \Psi V_4(t,u_{n-1}) + \vartheta \int_0^t V_4(s,u_{n-1})ds, \end{aligned} \tag{3.10}$$

with $x(0) = x_0$, $y(0) = y_0$, $z(0) = z_0$, and $u(0) = u_0$.

The difference between the successive terms is given as:

$$\begin{aligned} \tau_{1n} &= x_n(t) - x_{n-1}(t) = \Psi[V_1(t,x_{n-1}) - V_1(t,x_{n-2})] + \vartheta \int_0^t [V_1(s,x_{n-1}) - V_1(s,x_{n-2})]ds, \\ \tau_{2n} &= y_n(t) - y_{n-1}(t) = \Psi[V_2(t,y_{n-1}) - V_2(t,y_{n-2})] + \vartheta \int_0^t [V_2(s,y_{n-1}) - V_2(s,y_{n-2})]ds, \\ \tau_{3n} &= z_n(t) - z_{n-1}(t) = \Psi[V_3(t,z_{n-1}) - V_3(t,z_{n-2})] + \vartheta \int_0^t [V_3(s,z_{n-1}) - V_3(s,z_{n-2})]ds, \\ \tau_{4n} &= u_n(t) - u_{n-1}(t) = \Psi[V_4(t,u_{n-1}) - V_4(t,u_{n-2})] + \vartheta \int_0^t [V_4(s,u_{n-1}) - V_4(s,u_{n-2})]ds. \end{aligned} \tag{3.11}$$

Note that

$$x_n(t) = \sum_{i=1}^{n} \tau_{1i}(t),\ \ y_n(t) = \sum_{i=1}^{n} \tau_{2i}(t),\ \ z_n(t) = \sum_{i=1}^{n} \tau_{3i}(t),\ \ u_n(t) = \sum_{i=1}^{n} \tau_{4i}(t). \tag{3.12}$$

Proceeding in a similar manner, we will evaluate

$$\begin{aligned} \|\tau_{1n}(t)\| &= \|x_n(t) - x_{n-1}(t)\| \\ &= \left\| \Psi[V_1(t,x_{n-1}) - V_1(t,x_{n-2})] + \vartheta \int_0^t [V_1(s,x_{n-1}) - V_1(s,x_{n-2})]ds \right\|. \end{aligned} \tag{3.13}$$

Applying the triangular inequality on Eq (3.13) gives:

$$\|x_n(t) - x_{n-1}(t)\| \leq \Psi \|[V_1(t,x_{n-1}) - V_1(t,x_{n-2})]\| + \vartheta \int_0^t \|[V_1(s,x_{n-1}) - V_1(s,x_{n-2})]ds\|. \tag{3.14}$$

Since the function $V_1(x,t)$ satisfies the Lipschtiz condition, we have:

$$\|x_n(t) - x_{n-1}(t)\| \leq \Psi k_1 \|x_{n-1}) - x_{n-2}]\| + \vartheta k_1 \left\| \int_0^t [V_1(s, x_{n-1}) - V_1(s, x_{n-2})] ds \right\|. \tag{3.15}$$

This gives

$$\|\tau_{1n}(t)\| \leq \Psi k_1 \left\|\tau_{1(n-1)}(t)\right\| + \vartheta k_1 \int_0^t \left\|\tau_{1(n-1)}(s)\right\| ds. \tag{3.16}$$

The following results can be obtained by proceeding the same approach

$$\begin{aligned}
\|\tau_{2n}(t)\| &\leq \Psi k_2 \left\|\tau_{2(n-1)}(t)\right\| + \vartheta k_2 \int_0^t \left\|\tau_{2(n-1)}(s)\right\| ds, \\
\|\tau_{3n}(t)\| &\leq \Psi k_3 \left\|\tau_{3(n-1)}(t)\right\| + \vartheta k_3 \int_0^t \left\|\tau_{3(n-1)}(s)\right\| ds, \\
\|\tau_{4n}(t)\| &\leq \Psi k_4 \left\|\tau_{4(n-1)}(t)\right\| + \vartheta k_4 \int_0^t \left\|\tau_{4(n-1)}(s)\right\| ds.
\end{aligned} \tag{3.17}$$

Theorem 2. *The fractional order hyperchaotic sysyem* (3.1) *has a solution, if we are able to find* t_0 *with the following constraint:*

$$\Psi k_i + \vartheta k_i t_0 < 1, \quad i = 1, 2, 3, 4.$$

Proof. As proved that the Lipschtiz condition holds for $V_1(t,x)$, $V_2(t,y)$, $V_3(t,z)$, $V_4(t,u)$. Therefore, from Eqs (3.16) and (3.17), using the recursive method, we have:

$$\begin{aligned}
\|\tau_{1n}(t)\| &\leq \|x_n(0)\| \ [\Psi k_1 + \vartheta k_1 t]^n, \\
\|\tau_{2n}(t)\| &\leq \|y_n(0)\| \ [\Psi k_2 + \vartheta k_2 t]^n, \\
\|\tau_{3n}(t)\| &\leq \|z_n(0)\| \ [\Psi k_3 + \vartheta k_3 t]^n, \\
\|\tau_{4n}(t)\| &\leq \|u_n(0)\| \ [\Psi k_4 + \vartheta k_4 t]^n.
\end{aligned} \tag{3.18}$$

This confirms that the previously mentioned solutions do indeed exist. Furthermore, to validate that the specified functions are solutions of the fractional order hyperchaotic system with the Caputo-Fabrizio derivative, let us assume

$$\begin{aligned}
W_n &= x_n(t) - (x(t) - x(0)), \\
G_n &= y_n(t) - (y(t) - y(0)), \\
H_n &= z_n(t) - (z(t) - z(0)), \\
E_n &= u_n(t) - (u(t) - u(0)).
\end{aligned} \tag{3.19}$$

So then,

$$\begin{aligned}
x(t) - x(0) &= x_n(t) - W_n(t), \\
y(t) - y(0) &= y_n(t) - G_n(t), \\
z(t) - z(0) &= z_n(t) - H_n(t),
\end{aligned}$$

$$u(t) - u(0) = u_n(t) - E_n(t). \tag{3.20}$$

Therefore,

$$\begin{aligned} \|W_n(t)\| &= \left\| \Psi[V_1(t, x_n) - V_1(t, x_{n-1})] + \vartheta \int_0^t [V_1(s, x_n) - V_1(s, x_{n-1})] ds \right\| \\ &\leq \Psi \, \|V_1(t, x_n) - V_1(t, x_{n-1})\| + \vartheta \int_0^t \|V_1(s, x_n) - V_1(s, x_{n-1})\| \, ds \\ &\leq \Psi \; k_1 \, \|x_n - x_{n-1}\| + \vartheta k_1 \, \|x_n - x_{n-1}\| \, t. \end{aligned} \tag{3.21}$$

Applying the results in a recursive manner gives

$$\|W_n(t)\| \leq (\Psi + \vartheta \; t)^{n+1} \; k_1^{n+1}. \tag{3.22}$$

Then, at t_0 we have:

$$\|W_n\|_{t=t_0} \leq (\Psi + \vartheta \; t_0)^{n+1} \; k_1^{n+1}. \tag{3.23}$$

At $n \to \infty$ in Eq (3.23),

$$\|W_n(t)\| \to 0.$$

In the similar manner,

$$\|G_n(t)\| \to 0, \|H_n(t)\| \to 0, \|E_n(t)\| \to 0.$$

Further, to establish the uniqueness of the solution for the system (3.1), we assume that there exists another solution to this system, given by x_1, y_1, z_1, u_1. Then,

$$x(t) - x_1(t) = \Psi[V_1(t, x) - V_1(t, x_1)] + \vartheta \int_0^t [V_1(s, x) - V_1(s, x_1)] ds. \tag{3.24}$$

Taking norm on Eq (3.24) gives:

$$\|x(t) - x_1(t)\| \leq \Psi \, \|[V_1(t, x) - V_1(t, x_1)]\| + \vartheta \int_0^t \|[V_1(s, x) - V_1(s, x_1)]\| \, ds. \tag{3.25}$$

As $V_1(t, x)$ satisfies the Lipschtiz condition, we have

$$\|x(t) - x_1(t)\| \leq \Psi k_1 \, \|[x(t) - x_1(t)]\| + \vartheta \int_0^t k_1 \quad \|x(t) - x_1(t)]\| \, ds, \tag{3.26}$$

which gives

$$\|x(t) - x_1(t)\| \, (1 - \Psi \; k_1 - \vartheta \; k_1 \, t) \leq 0. \tag{3.27}$$

□

Theorem 3. *If the condition given below holds, then the hyperchaotic system has a unique solution*

$$(1 - \Psi \; k_1 - \vartheta \; k_1 \, t) > 0. \tag{3.28}$$

Proof. From Eq (3.27), we have

$$\|x(t) - x_1(t)\| (1 - \Psi\ k_1 - \vartheta\ k_1\, t) \leq 0,$$

and if the following also holds:

$$(1 - \Psi\ k_1 - \vartheta\ k_1\, t) > 0,$$

then this is possible only if

$$\|x(t) - x_1(t)\| = 0.$$

Hence, $x(t) = x_1(t)$. Similarly, $y(t) = y_1(t)$, $z(t) = z_1(t)$, and $u(t) = u_1(t)$. □

3.2. Numerical solutions for defined model

To solve the fractional order 4D hyperchaotic system with the Caputo-Fabrizio derivative numerically, we follow the method as briefed in [49].

Consider the 4D hyperchaotic system with the Caputo-Fabrizio derivative of fractional order ε, $0 < \varepsilon < 1$,

$$\begin{aligned}
{}_0^{CF}\mathbb{D}_0^{\varepsilon(t)}\{x(t)\} &= a\,(y - x) + u, & x(0) &= x_0,\\
{}_0^{CF}\mathbb{D}_0^{\varepsilon(t)}\{y(t)\} &= c\,y - 10\,x\,z, & y(0) &= y_0,\\
{}_0^{CF}\mathbb{D}_0^{\varepsilon(t)}\{z(t)\} &= -b\,z + 10\,x\,y, & z(0) &= z_0,\\
{}_0^{CF}\mathbb{D}_0^{\varepsilon(t)}\{u(t)\} &= d\,y + x^2, & u(0) &= u_0.
\end{aligned} \tag{3.29}$$

We take into account the following general equation:

$${}^{CF}\mathbb{D}_t^{\varepsilon} P(t) = \omega(t, P(t)), \quad t \geq 0, \quad P(0) = P_0, \tag{3.30}$$

where $P(t) = \{x(t), y(t), z(t), u(t)\}$, and $P(0) = \{x(0), y(0), z(0), u(0)\}$.

Proceeding as referred in [50], we rewrite Eq (3.30) as

$$P(t) - P(0) = \frac{1-\varepsilon}{M(\varepsilon)}\omega(t, P(t)) + \frac{\varepsilon}{Q(\varepsilon)}\int_0^t \omega\,(s, P(s))ds. \tag{3.31}$$

At $t = t_{n+1}$, Eq (3.31) is written as

$$P(t_{n+1}) - P(0) = \frac{1-\varepsilon}{Q(\varepsilon)}\omega(t_n, P(t_n)) + \frac{\varepsilon}{Q(\varepsilon)}\int_0^{t_{n+1}} \omega(s, P(s))ds. \tag{3.32}$$

Also at $t = t_n$, Eq (3.31) gives

$$P(t_n) - P(0) = \frac{1-\varepsilon}{Q(\varepsilon)}\omega\,(t_{n-1}, P(t_{n-1})) + \frac{\varepsilon}{Q(\varepsilon)}\int_0^{t_n} \omega\,(s, P(s))ds. \tag{3.33}$$

From Eqs (3.32) and (3.33), we get

$$P(t_{n+1}) - P(t_n) = \frac{1-\varepsilon}{Q(\varepsilon)}[\omega\,(t_n, P(t_n)) - \omega\,(t_{n-1}, P(t_{n-1}))] + \frac{\varepsilon}{Q(\varepsilon)}\int_{t_n}^{t_{n+1}} \omega(s, P(s))ds. \tag{3.34}$$

Lagrange polynomial interpolation on $\omega(s, P(s))$ gives

$$\omega\left(s, P(s)\right) = \frac{s - t_{m-1}}{t_m - t_{m-1}}\,\omega\left(t_m, P_{t_m}\right) + \frac{s - t_m}{t_{m-1} - t_m}\,\omega\left(t_{m-1}, P_{t_{m-1}}\right). \tag{3.35}$$

Substituting $\omega\left(s, P(s)\right)$ in Eq (3.34) gives

$$P_{n+1} - P_n = \frac{1-\varepsilon}{Q(\varepsilon)}[\omega\left(t_n, P(t_n)\right) - \omega\left(t_{n-1}, P(t_{n-1})\right)] + \frac{\varepsilon}{Q(\varepsilon)} \int_{t_n}^{t_{n+1}} \left(\frac{\omega\left(t_n, P_n\right)}{h}(s - t_{n-1}) - \frac{\omega\left(t_{n-1}, P_{n-1}\right)}{h}(s - t_n)\right) ds. \tag{3.36}$$

On taking $h = t_n - t_{n-1}$ and solving, we get

$$P_{n+1} = P_0 + \left(\frac{1-\varepsilon}{Q(\varepsilon)} + \frac{3h}{2\ Q(\varepsilon)}\right)\omega\left(t_n, P(t_n)\right) - \left(\frac{1-\varepsilon}{Q(\varepsilon)} + \frac{\varepsilon\ h}{2\ Q(\varepsilon)}\right)\omega(t_{n-1}, P(t_{n-1})). \tag{3.37}$$

In a similar way, we have

$$x_{n+1} = x_0 + \left(\frac{1-\varepsilon}{Q(\varepsilon)} + \frac{3h}{2\ Q(\varepsilon)}\right)V_1(t_n, x(t_n)) - \left(\frac{1-\varepsilon}{Q(\varepsilon)} + \frac{\varepsilon\ h}{2\ Q(\varepsilon)}\right)V_1(t_{n-1}, x(t_{n-1})), \tag{3.38}$$

where $V_1(t, x) = a\,(y - x) + u$.

$$y_{n+1} = y_0 + \left(\frac{1-\varepsilon}{Q(\varepsilon)} + \frac{3h}{2\ Q(\varepsilon)}\right)V_2(t_n, y(t_n)) - \left(\frac{1-\varepsilon}{Q(\varepsilon)} + \frac{\varepsilon\ h}{2\ Q(\varepsilon)}\right)V_2(t_{n-1}, y(t_{n-1})), \tag{3.39}$$

where $V_2(t, y) = c\,y - 10\,x\,z$.

$$z_{n+1} = z_0 + \left(\frac{1-\varepsilon}{Q(\varepsilon)} + \frac{3h}{2\ Q(\varepsilon)}\right)V_3(t_n, z(t_n)) - \left(\frac{1-\varepsilon}{Q(\varepsilon)} + \frac{\varepsilon\ h}{2\ Q(\varepsilon)}\right)V_3(t_{n-1}, z(t_{n-1})), \tag{3.40}$$

where $V_3(t, z) = -b\,z + 10\,x\,y$.

$$u_{n+1} = u_0 + \left(\frac{1-\varepsilon}{Q(\varepsilon)} + \frac{3h}{2\ Q(\varepsilon)}\right)V_4(t_n, u(t_n)) - \left(\frac{1-\varepsilon}{Q(\varepsilon)} + \frac{\varepsilon\ h}{2\ Q(\varepsilon)}\right)V_4(t_{n-1}, u(t_{n-1})), \tag{3.41}$$

where, $V_4(t, u) = d\,y + x^2$.

The numerical solutions of the fractional order 4D hyperchaotic system with the Caputo-Fabrizio derivative defined by Eq (3.1) are obtained from Eqs (3.38)–(3.41).

3.3. Simulations

The simulations are performed for different fractional orders. The parameter values [47] are taken as $a = 35, b = 3, c = 12$. The initial conditions are taken as $x(0) = y(0) = z(0) = u(0) = 1$. Further, we consider three different values for the variable parameter d (10, 17, and 22).

- In Figures 1–3, the numerical simulations are performed for the fractional order $\varepsilon = 0.95$, 0.97, and 0.99, respectively, with $d = 10$.

- In Figures 4–6, the numerical simulations are performed for the fractional order $\varepsilon = 0.95$, 0.97, and 0.99, respectively, with $d = 17$.
- In Figures 7–9, the numerical simulations are performed for the fractional order $\varepsilon = 0.95$, 0.97, and 0.99, respectively, with $d = 22$.

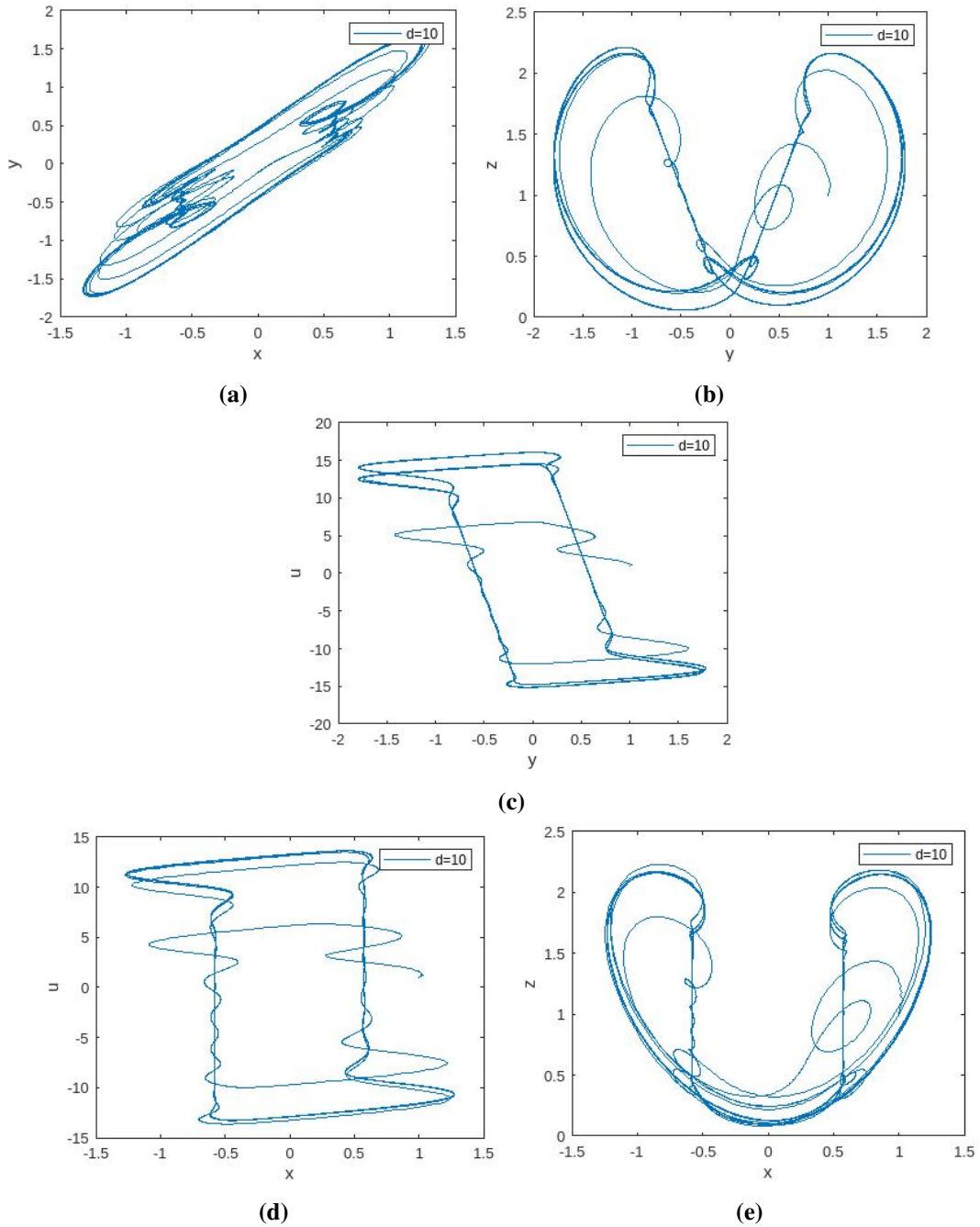

Figure 1. Phase portrait of the 4D fractional order Caputo-Fabrizio hyperchaotic system defined by Eq (3.1) simulated at $\varepsilon = 0.95$ with $a = 35$, $b = 3$, $c = 12$, $d = 10$.

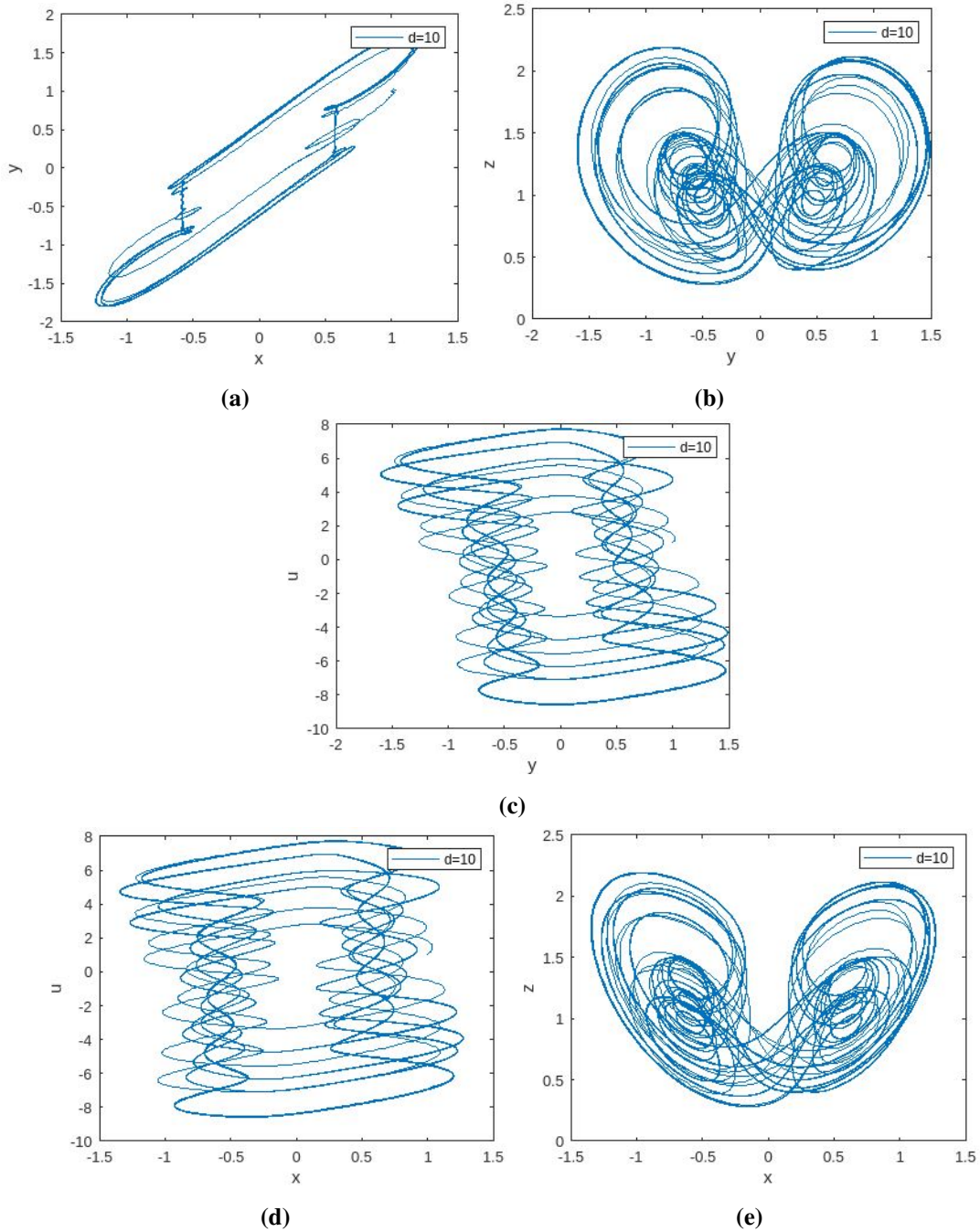

Figure 2. Phase portrait of the 4D fractional order Caputo-Fabrizio hyperchaotic system defined by Eq (3.1) simulated at $\varepsilon = 0.97$ with $a = 35$, $b = 3$, $c = 12$, $d = 10$.

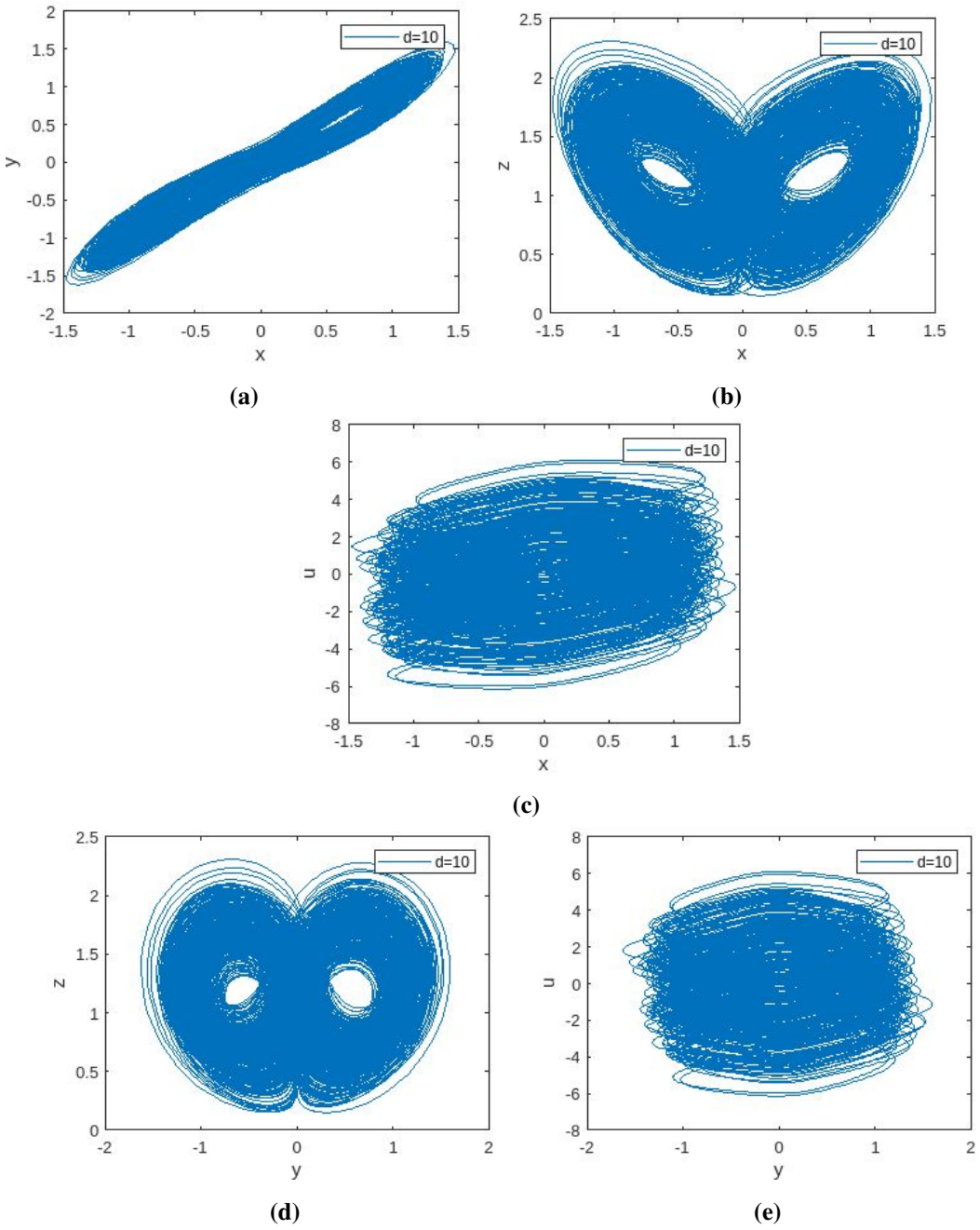

Figure 3. Phase portrait of the 4D fractional order Caputo-Fabrizio hyperchaotic system defined by Eq (3.1) simulated at $\varepsilon = 0.99$ with $a = 35$, $b = 3$, $c = 12$, $d = 10$.

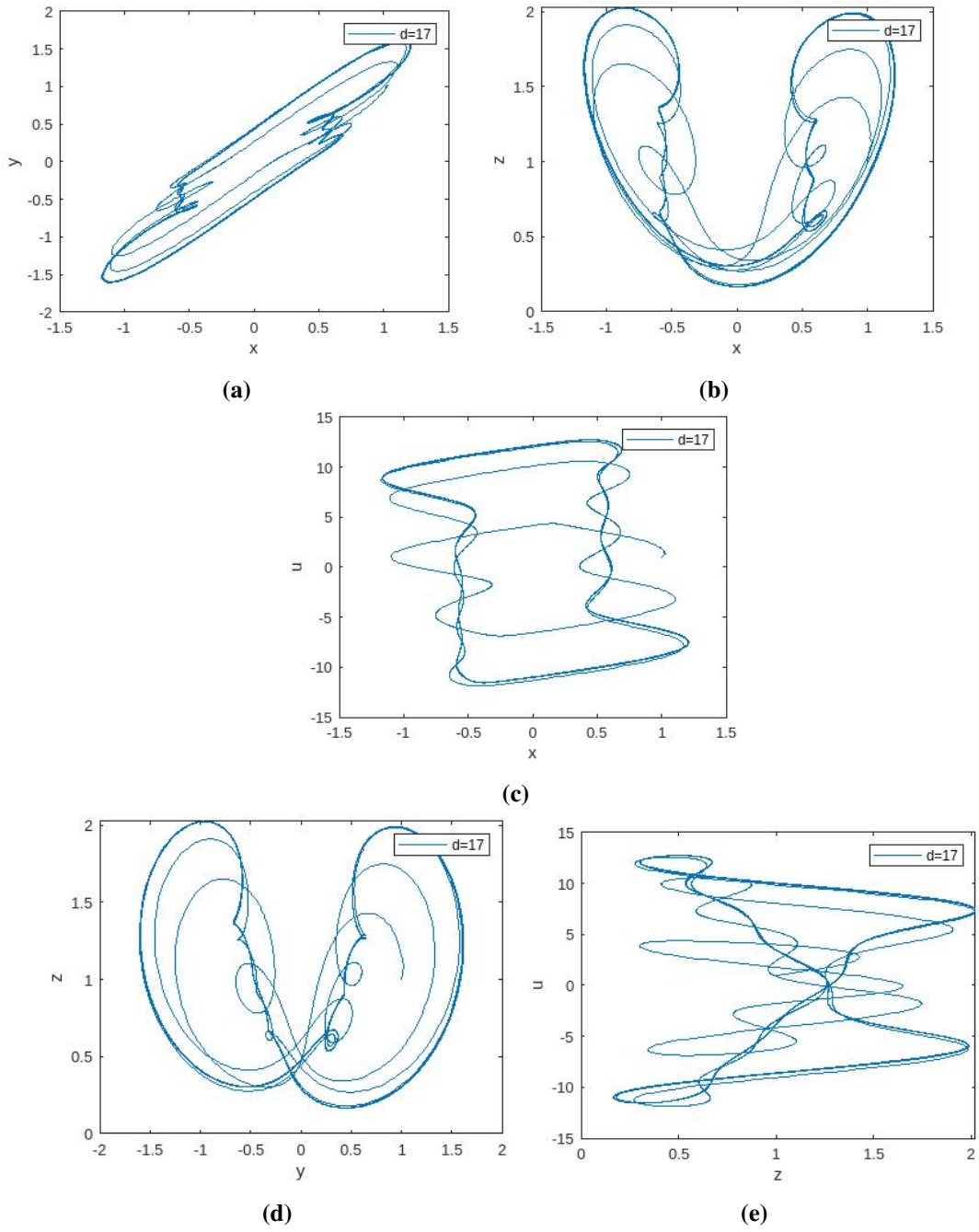

Figure 4. Phase portrait of the 4D fractional order Caputo-Fabrizio hyperchaotic system defined by Eq (3.1) simulated at $\varepsilon = 0.95$ with $a = 35$, $b = 3$, $c = 12$, $d = 17$.

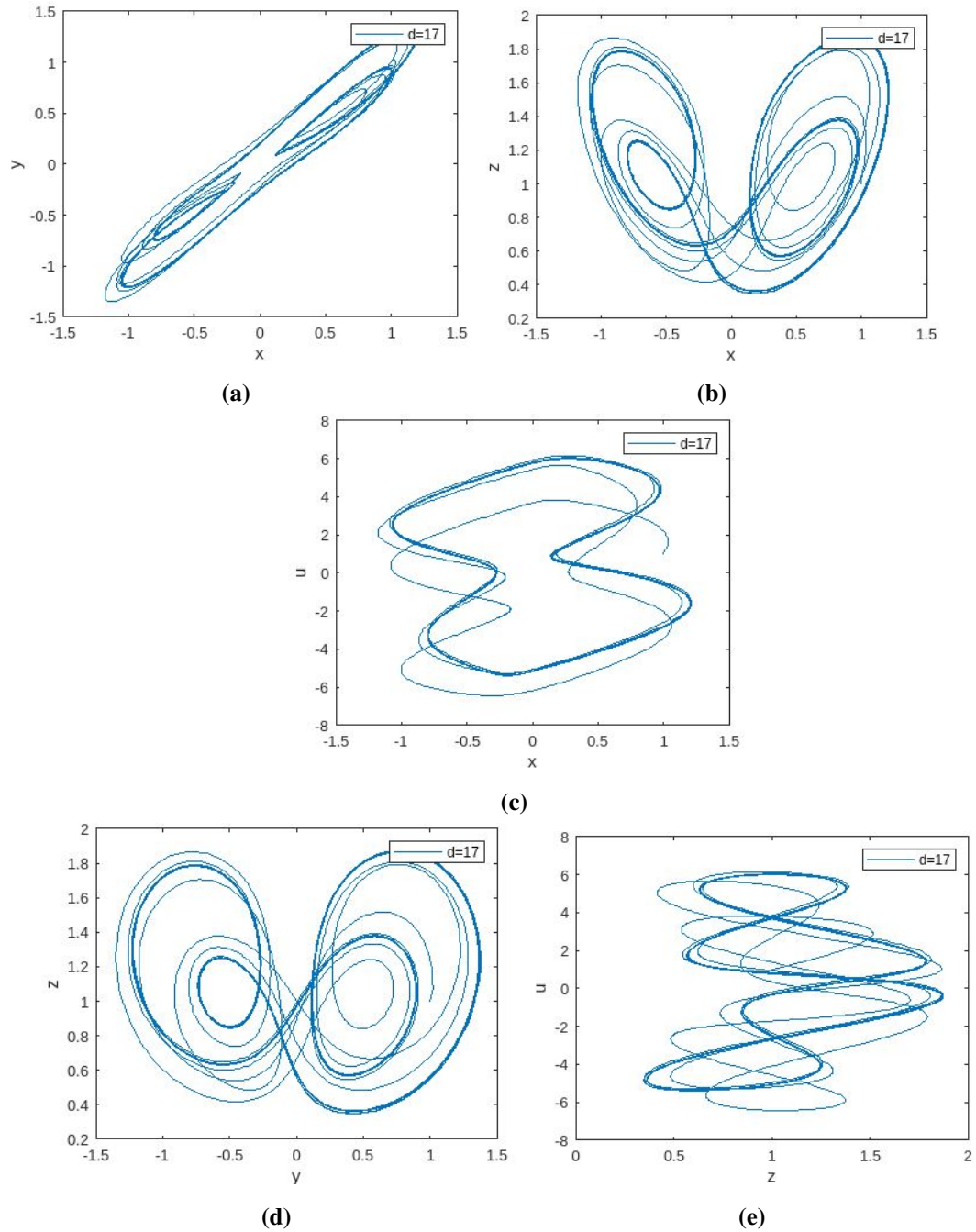

Figure 5. Phase portrait of the 4D fractional order Caputo-Fabrizio hyperchaotic system defined by Eq (3.1) simulated at $\varepsilon = 0.97$ with $a = 35$, $b = 3$, $c = 12$, $d = 17$.

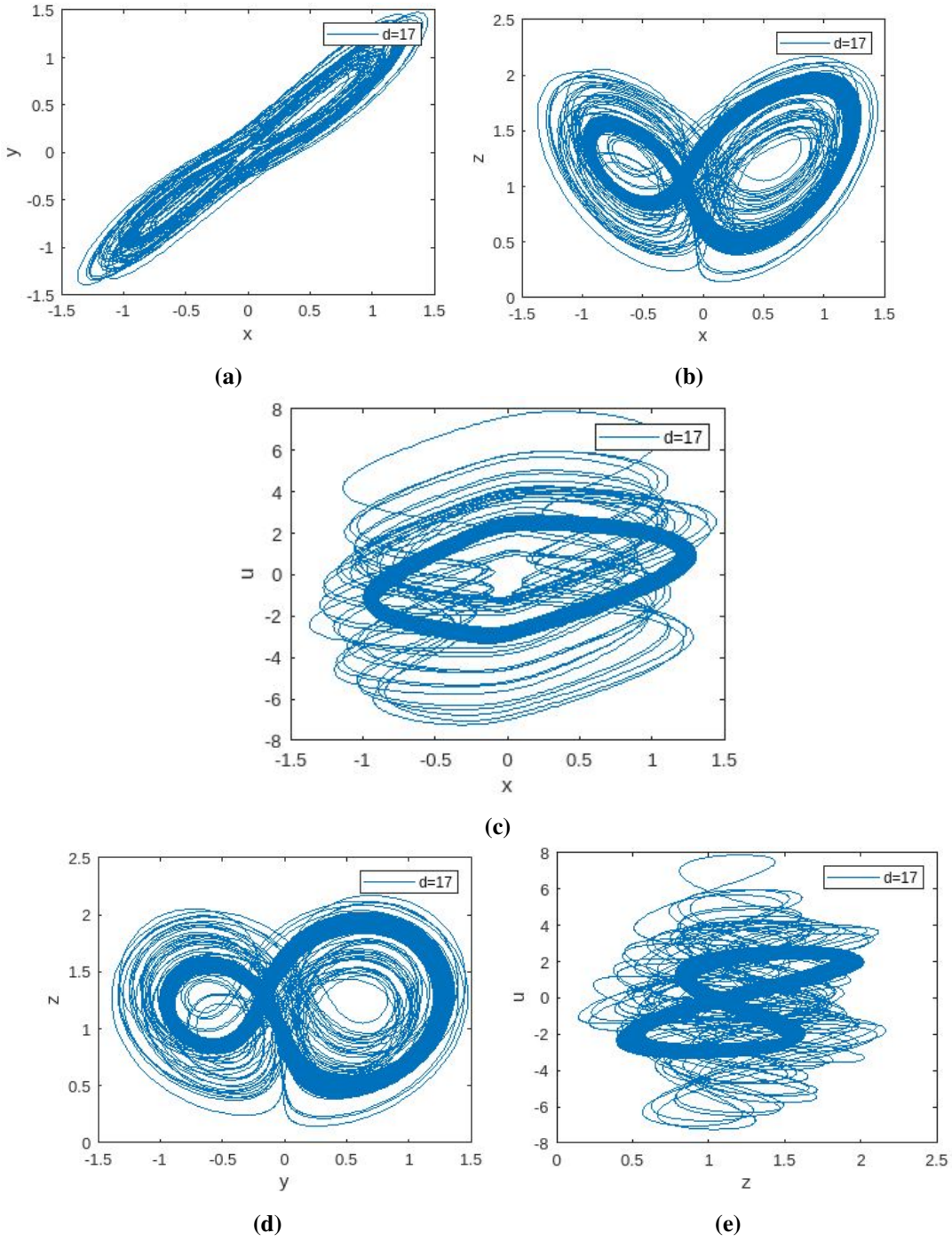

Figure 6. Phase portrait of the 4D fractional order Caputo-Fabrizio hyperchaotic system defined by Eq (3.1) simulated at $\varepsilon = 0.99$ with $a = 35$, $b = 3$, $c = 12$, $d = 17$.

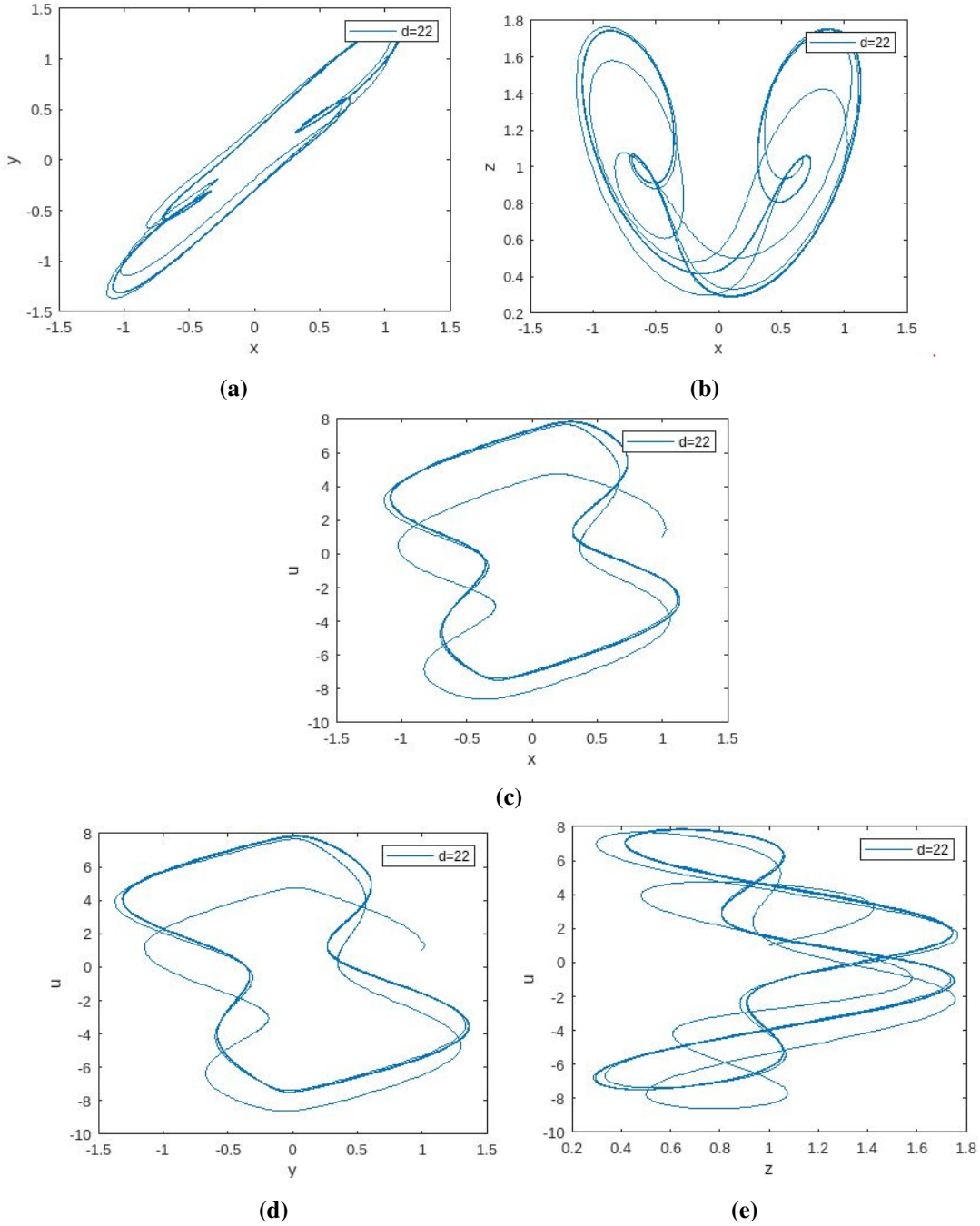

Figure 7. Phase portrait of the 4D fractional order Caputo-Fabrizio hyperchaotic system defined by Eq (3.1) simulated at $\varepsilon = 0.95$ with $a = 35$, $b = 3$, $c = 12$, $d = 22$.

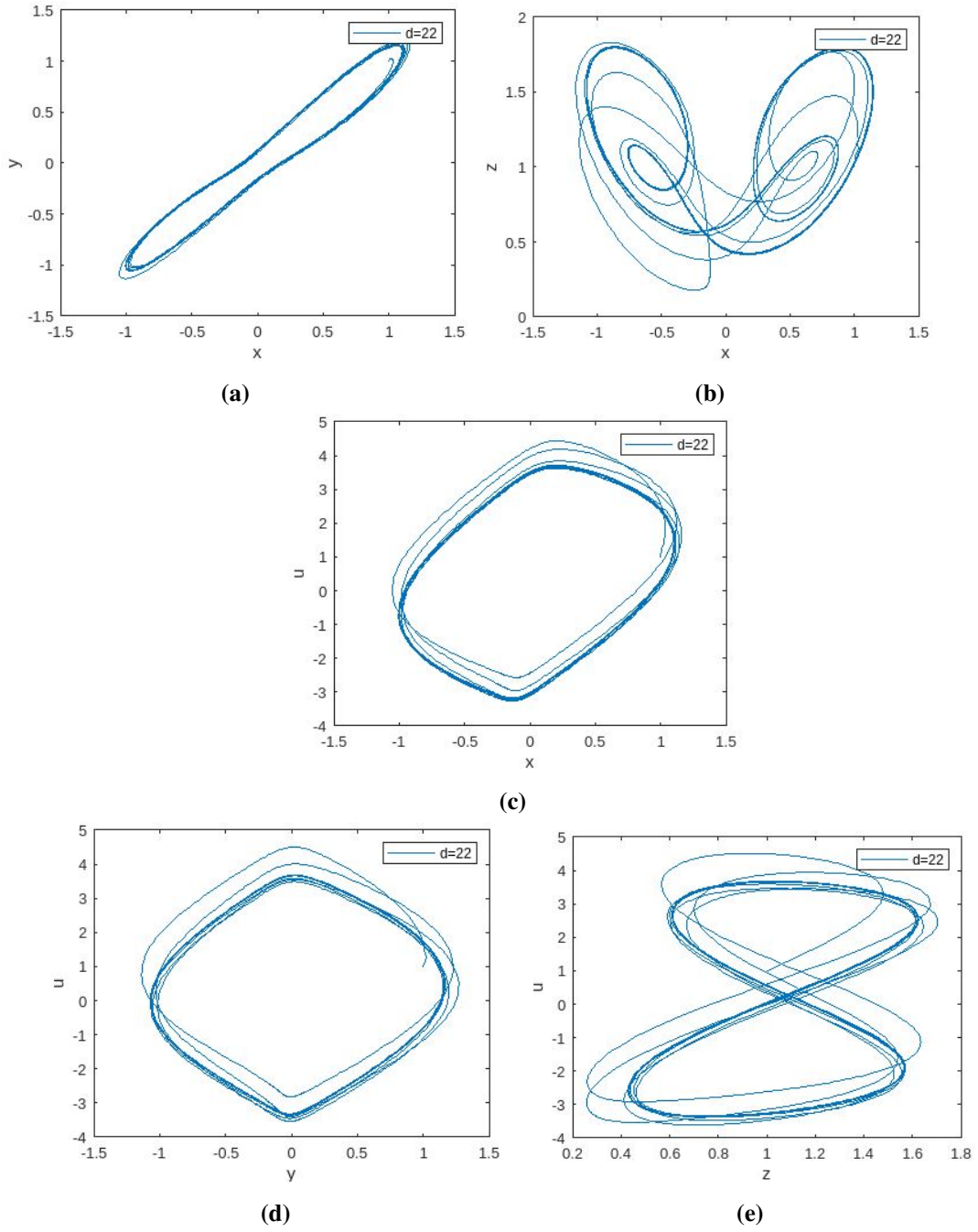

Figure 8. Phase portrait of the 4D fractional order Caputo-Fabrizio hyperchaotic system defined by Eq (3.1) simulated at $\varepsilon = 0.97$ with $a = 35$, $b = 3$, $c = 12$, $d = 22$.

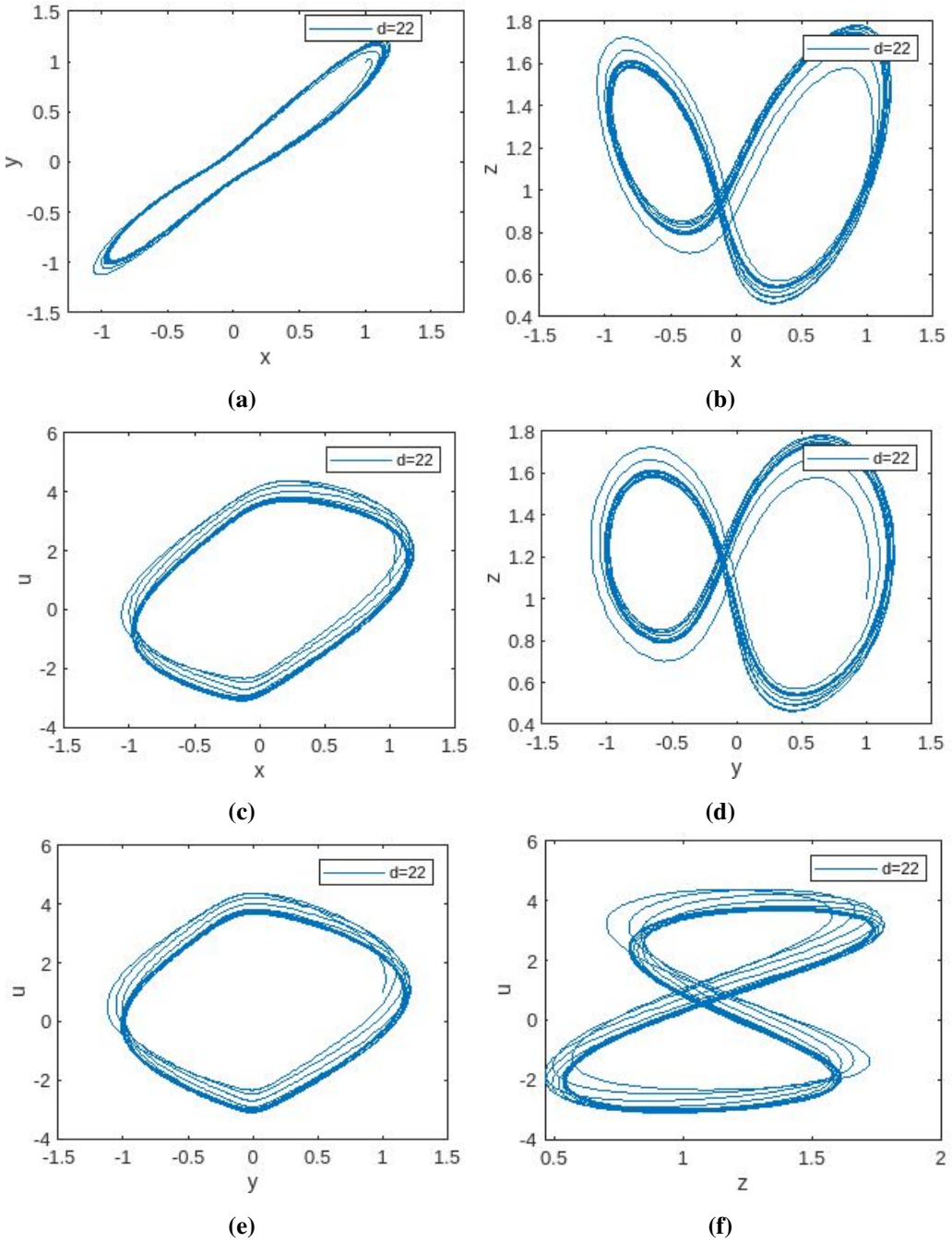

Figure 9. Phase portrait of the 4D fractional order Caputo-Fabrizio hyperchaotic system defined by Eq (3.1) simulated at $\varepsilon = 0.99$ with $a = 35$, $b = 3$, $c = 12$, $d = 22$.

4. Circuit implementation of the hyperchaotic system

This part of our research delves into the practical realm by constructing analog circuits that implement our hyperchaotic system enabling experimental validation. Starting with the theoretical basis established by the system (3.1), we methodically transform these theoretical equations into practical circuit implementations. Translating the hyperchaotic system into physical circuits

necessitates meticulous attention to the behavioral dynamics of the system, verifying the results accurately. This reflects the fundamentals of the theoretical system truthfully, replicating its chaotic behavior. Our goal is to close the gap between theory and practical implementation, therefore, offering a strong interface for observation and investigation.

In this research, the circuit is designed using operational amplifiers (LF353N), resistors, multipliers (AD633), and capacitors all powered by a ±15 V supply. The circuit analysis equations, derived from the hyperchaotic system, are detailed in [47]. The circuit diagrams representing the hyperchaotic system are as follows in Figures 10–14:

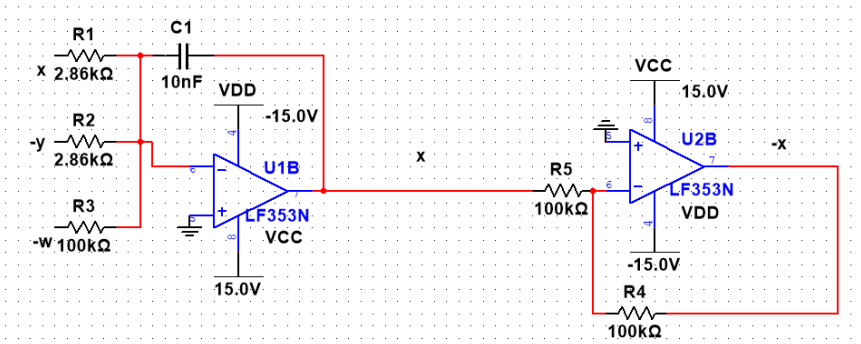

Figure 10. Representation of the variable x through circuit diagram.

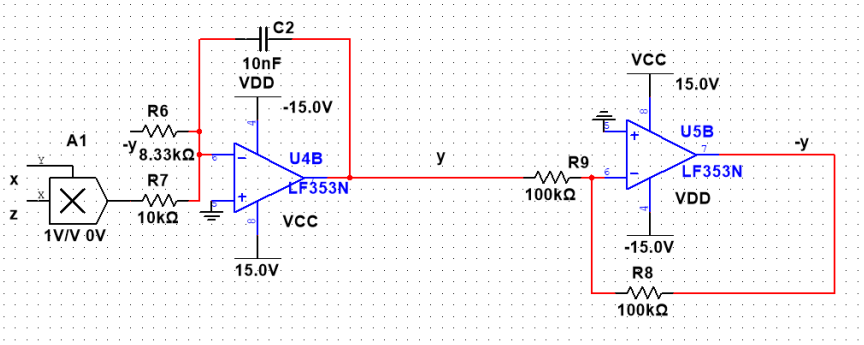

Figure 11. Representation of the variable y through circuit diagram.

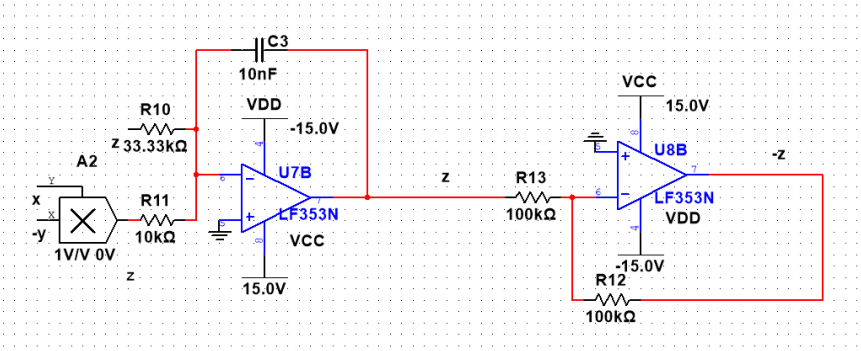

Figure 12. Representation of the variable z through circuit diagram.

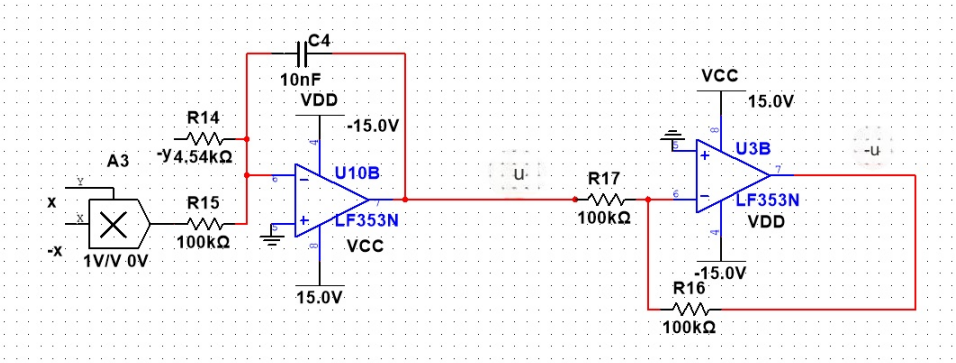

Figure 13. Representation of the variable u through circuit diagram.

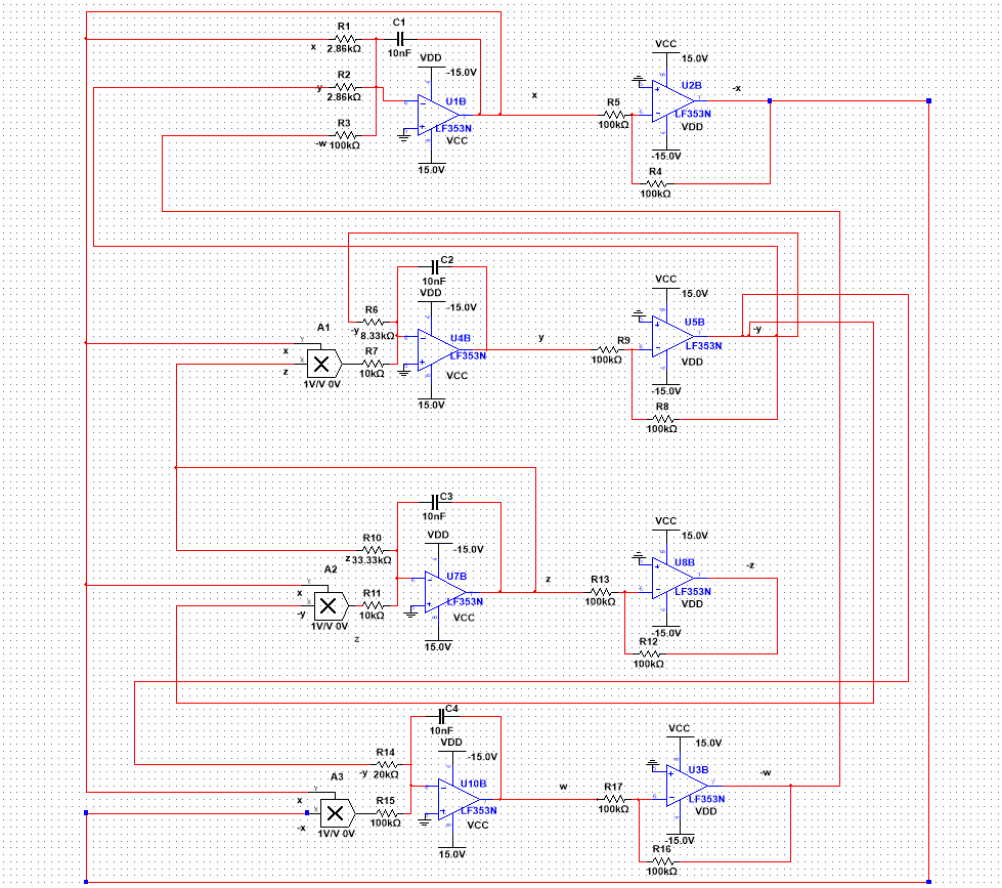

Figure 14. Feedback circuit representing the hyperchaotic system.

Figure 15 show the chaotic behavior of the hyperchaotic system obtained through circuit implemetation using Multisim. Further, figures 16-19 show the comparison between the phase portrait behavior of the hyperchaotic system at fractional order $\epsilon = 0.99$ and the chaotic behavior of the hyperchaotic system through circuit realization simulated by Multisim.

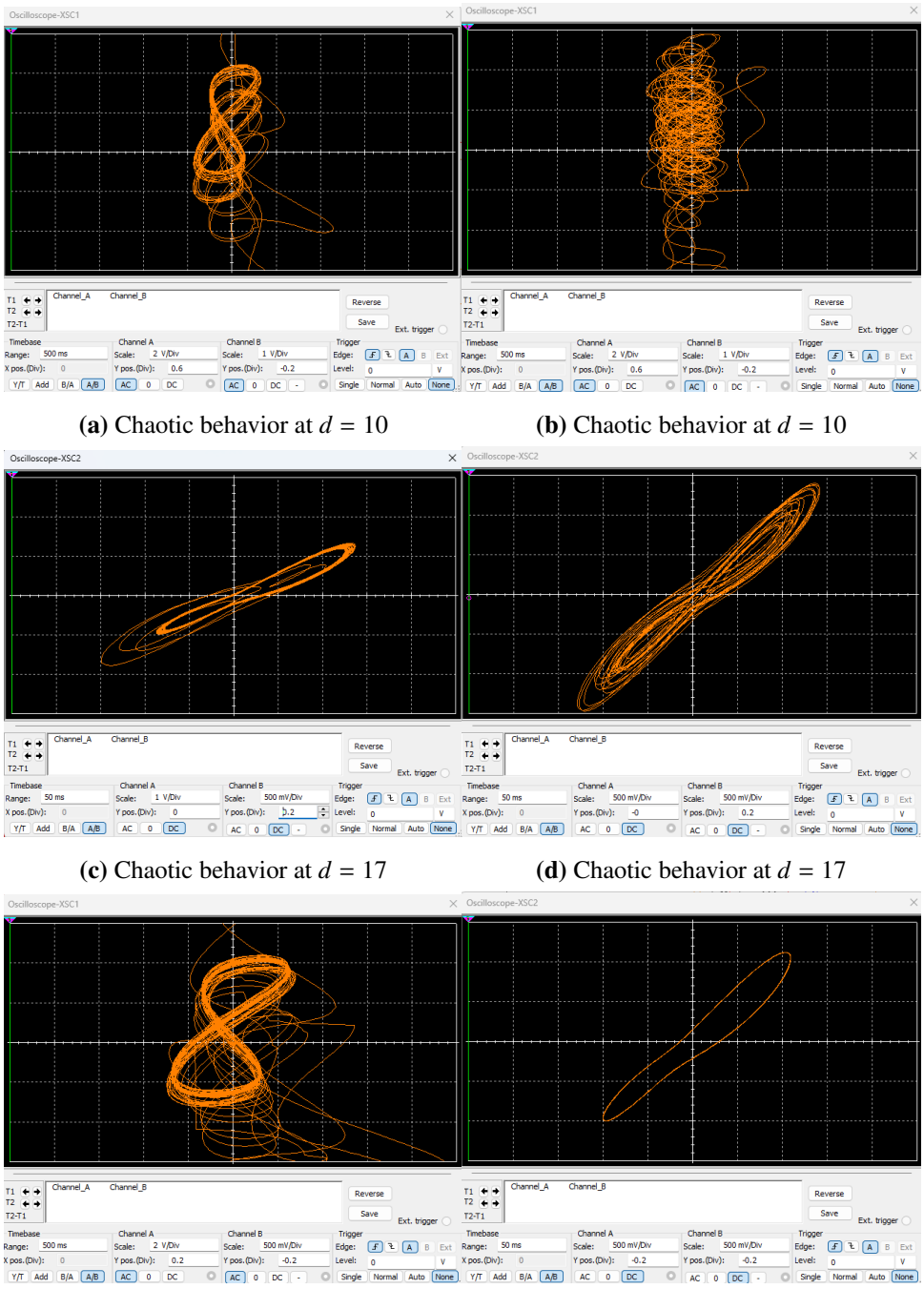

(a) Chaotic behavior at $d = 10$ **(b)** Chaotic behavior at $d = 10$

(c) Chaotic behavior at $d = 17$ **(d)** Chaotic behavior at $d = 17$

(e) Chaotic behavior at $d = 22$ **(f)** Chaotic behavior at $d = 22$

Figure 15. Chaotic behavior of circuit implementation of hyperchaotic system simulated by Multisim at distinct values of the variable parameter d.

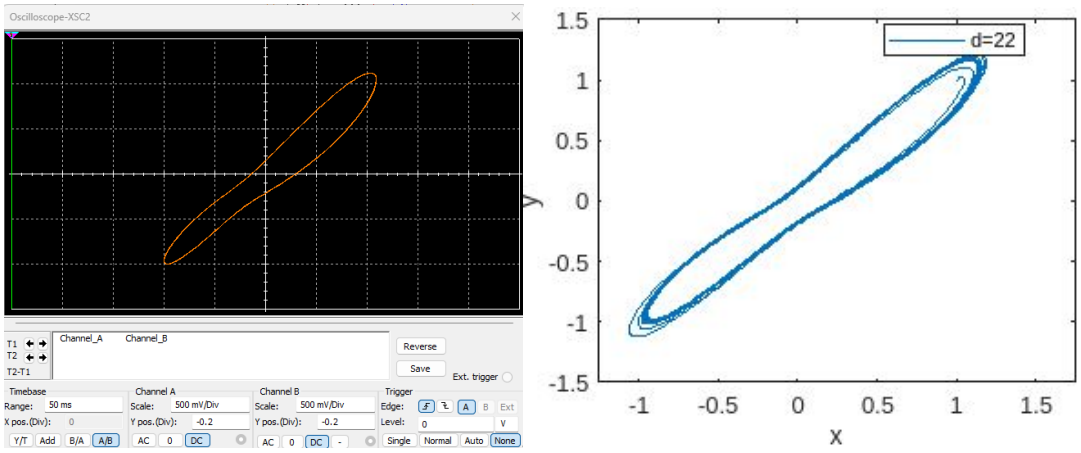

(a) Chaotic behavior through circuit realization simulated by Multisim

(b) Phase portrait behavior of fractional Caputo-Fabrizio hyperchaotic system

Figure 16. Phase portrait behavior of the defined model at $\varepsilon = 0.99$ and the chaotic behavior of the hyperchaotic system through circuit realization simulated by Multisim.

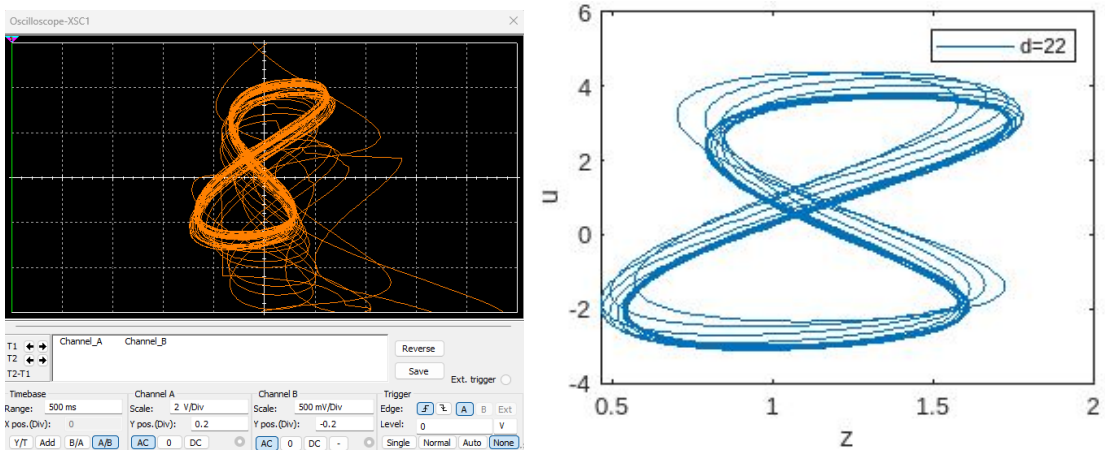

(a) Chaotic behavior through circuit realization simulated by Multisim

(b) Phase portrait behavior of fractional Caputo-Fabrizio hyperchaotic system

Figure 17. Phase portrait behavior of the model for fractional order $\varepsilon = 0.99$ and the chaotic behavior of the hyperchaotic system through circuit realization simulated by Multisim.

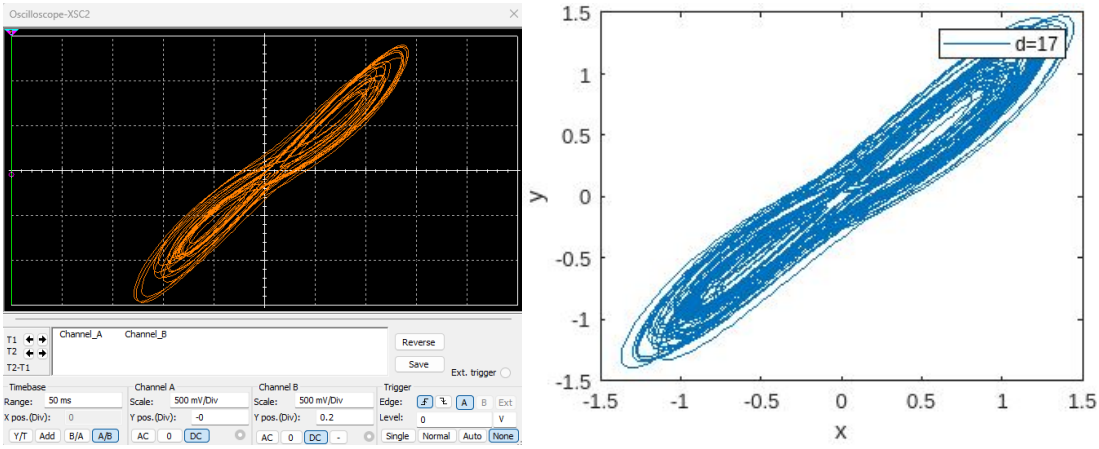

(a) Chaotic behavior through circuit realization simulated by Multisim

(b) Phase portrait behavior of fractional Caputo-Fabrizio hyperchaotic system

Figure 18. Phase portrait behavior of the model for fractional order $\varepsilon = 0.99$ and the chaotic behavior of the hyperchaotic system through circuit realization simulated by Multisim.

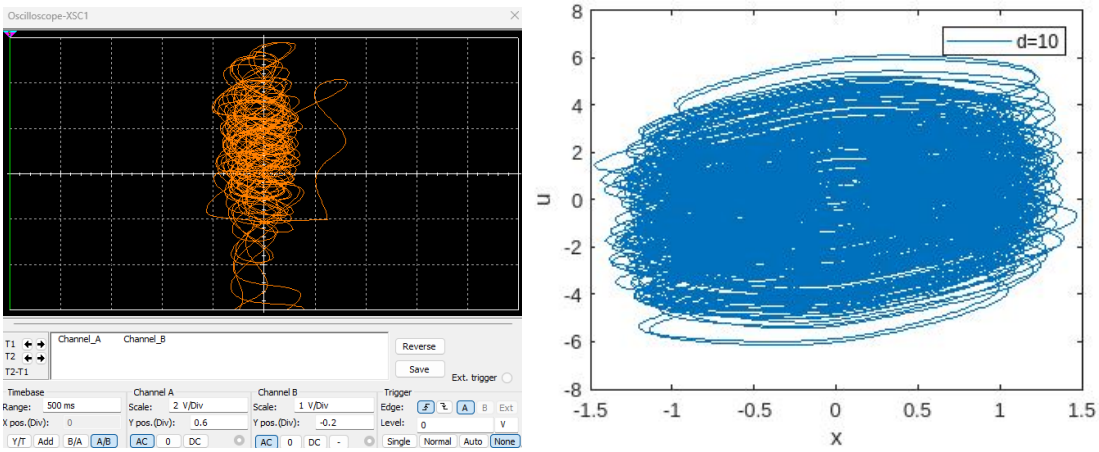

(a) Chaotic behavior through circuit realization simulated by Multisim

(b) Phase portrait behavior of fractional Caputo-Fabrizio hyperchaotic system

Figure 19. Phase portrait behavior of the model for fractional order $\varepsilon = 0.99$ and the chaotic behavior of the hyperchaotic system through circuit realization simulated by Multisim.

5. Discussion on the results

As the parameter d in the hyperchaotic system defined by Eq (3.1) is chosen to be variable, so we consider three different values for d, i.e., $d = 10, 17$, and 22.

- Figures 1–9 show the simulations for the 4D fractional order Caputo-Fabrizio hyperchaotic system for $d = 10, 17, 22$ for different fractional orders $\varepsilon = 0.95, 0.97$, and 0.99.
- Figures 10–13 depict the circuit diagrams to represent the driving variables.
- Figure 14 depicts the feedback circuit to represent the hyperchaotic system.

- Figure 15 shows the chaotic behavior of circuit implementation of the hyperchaotic system simulated by Multisim for distinct values of d.
- Figures 16–19 show a comparison between the phase portrait behavior of the hyperchaotic system at fractional order $\varepsilon = 0.99$ and the chaotic behavior obtained as a result of circuit realization.
- The comparison observed from the Figures 16–19 show the compatibility of the fractional order Caputo-Fabrizio hyperchaotic system with the circuit realization for fractional order $\varepsilon = 0.99$.

6. Conclusions

This research extends a hyperchaotic system given by Eq (1.1) to fractional order using the Caputo-Fabrizio derivative. The existence of a unique solution for the 4D fractional order Caputo-Fabrizio hyperchaotic system given by Eq (3.1) is proved and this system is solved numerically. Figures 1–9 show the simulations that are performed for different fractional orders, i.e., $\varepsilon = 0.95, 0.97$, and 0.99. We have also designed analog circuits that implement our chaotic system, enabling experimental validation. Figures 10–13 depict the circuit diagrams to represent the driving variables, and Figure 14 depicts the feedback circuit to represent the hyperchaotic system. Figure 15 shows the chaotic behavior of circuit implementation of the hyperchaotic system simulated by Multisim for distinct values of d. From Figures 16–19, we observe the comparison between the phase portrait behavior of the hyperchaotic system for fractional order $\varepsilon = 0.99$ and the chaotic behavior obtained as a result of circuit realization. These figures show the compatibility of the fractional order Caputo-Fabrizio hyperchaotic system with the chaotic behavior obtained through circuit realization for fractional order $\varepsilon = 0.99$, hence, bridging a gap between simulation and real-world application. This subsequent circuit implementation revealed that the theoretical predictions closely match the experimental findings when $\varepsilon = 0.99$. The figures demonstrate the alignment between the theoretical and experimental outcomes. Fu et al. [47] demonstrated that the audio encryption method based on the hyperchaotic system (1.1) is viable and this approach can be applied to the encryption of audio, images, videos, and other data types. As fractional derivatives introduce increased complexity, this work demonstrates that fractional order hyperchaotic system (3.1) can offer stronger security. By showcasing the chaotic dynamics, we establish a foundation for future advancements in circuit integration and the development of complex control systems. Consequently, the findings of this research are expected to drive advancement in concepts and implementation across various scientific domains.

Author contributions

Shivani Sharma: Conceptualization, methodology, software, validation, formal analysis, investigation, writing-original draft preparation, visualization, writing-review and editing, supervision; A. M. Alqahtani: Methodology, validation, formal analysis, investigation, writing-original draft preparation, writing-review and editing; Arun Chaudhary: Methodology, validation, investigation, writing-review and editing, supervision; Aditya Sharma: Conceptualization, methodology, software, writing-original draft preparation, visualization, writing-review and editing. All authors have read and approved the final version of the manuscript for publication.

Use of Generative-AI tools declaration

The authors declare they have not used Artificial Intelligence (AI) tools in the creation of this article.

Acknowledgments

The authors are thankful to the editor and reviewer's for their suggestions in iproving this manuscript.

Conflict of interest

There is no conflict of interest declared by the authors.

References

1. K. B. Oldham, J. Spanier, *The fractional calculus: Theory and applications of differentiation and integration to arbitrary order*, Mathematics in Science and Engineering, Academic Press, **111** (1974).
2. M. Caputo, M. Fabrizio, A new definition of fractional derivative without singular kernel, *Prog. Fract. Differ. Appl.*, **1** (2015), 73–85. https://doi.org/10.12785/pfda/010201
3. A. Atangana, D. Baleanu, New fractional derivatives with nonlocal and nonsingular kernel: Theory and application to heat transfer model, *Therm. Sci.*, **20** (2016), 763–769. https://doi.org/10.2298/TSCI160111018A
4. A. B. M. Alzahrani, R. Saadeh, M. A. Abdoon, M. Elbadri, M. Berir, A. Qazza, Effective methods for numerical analysis of the simplest chaotic circuit model with Atangana-Baleanu Caputo fractional derivative, *J. Eng. Math.*, **144** (2024), 9. https://doi.org/10.1007/s10665-023-10319-x
5. L. Song, W. Yu, Y. Tan, K. Duan, Calculations of fractional derivative option pricing models based on neural network, *J. Comput. Appl. Math.*, **437** (2024), 115462. https://doi.org/10.1016/j.cam.2023.115462
6. A. M. Alqahtani, A. Chaudhary, R. S. Dubey, S. Sharma, Comparative analysis of the chaotic behavior of a five-dimensional fractional hyperchaotic system with constant and variable order, *Fractal Fract.*, **8** (2024), 421. https://doi.org/10.3390/fractalfract8070421
7. A. D. Matteo, P. D. Spanos, Determination of nonstationary stochastic response of linear oscillators with fractional derivative elements of rational Order, *ASME. J. Appl. Mech.*, **91** (2024), 041008. https://doi.org/10.1115/1.4064143
8. G. Barbero, L. R. Evangelista, R. S. Zola, E. K. Lenzi, A. M. Scarfone, A brief review of fractional calculus as a tool for applications in physics: Adsorption phenomena and electrical impedance in complex fluids, *Fractal Fract.*, **8** (2024), 369. https://doi.org/10.3390/fractalfract8070369
9. R. Wang, Y. Sui, Method for measuring the fractional derivative of a two-dimensional magnetic field based on Taylor-Riemann series, *Fractal Fract.*, **8** (2024), 375. https://doi.org/10.3390/fractalfract8070375

10. S. Sharma, R. S. Dubey, A. Chaudhary, Caputo fractional model for the predator-prey relation with sickness in prey and refuge to susceptible prey, *Int. J. Math. Ind.*, **1** (2024), 2450014. https://doi.org/10.1142/S266133522450014X

11. M. A. Almuqrin, P. Goswami, S. Sharma, I. Khan, R. S. Dubey, A. Khan, Fractional model of Ebola virus in population of bats in frame of Atangana-Baleanu fractional derivative, *Results Phys.*, **2**6 (2021), 104295. https://doi.org/10.1016/j.rinp.2021.104295

12. S. Althubiti, S. Sharma, P. Goswami, R. S. Dubey, Fractional SIAQR model with time dependent infection rate, *Arab J. Basic Appl. Sci.*, **30** (2023), 307–316. https://doi.org/10.1080/25765299.2023.2209981

13. B. B. Mandelbrot, Fractal geometry: What is it, and what does it do? *Proc. R. Soc. Lond.*, **423** (1989), 3–16. https://doi.org/10.1098/rspa.1989.0038

14. J. H. He, A new fractal derivation, *Therm. Sci.*, **15** (2011), 145–147. https://doi.org/10.2298/TSCI11S1145H

15. J. H. He, Y. O. El-DiB, A tutorial introduction to the two-scale fractal calculus and its application to the fractal Zhiber-Shabat Oscillator, *Fractals*, **29** (2021), 2150268. https://doi.org/10.1142/S0218348X21502686

16. C. H. He, H. Liu, C. Liu, A fractal-based approach to the mechanical properties of recycled aggregate concretes, *Facta. Univ.-Ser. Mech.*, **22** (2024), 329–342. https://doi.org/10.22190/fume240605035h

17. C. H. He, C. Liu, Fractal dimensions of a porous concrete and its effect on the concrete's strength, *Facta. Univ.-Ser. Mech.*, **21** (2023), 137–150. https://doi.org/10.22190/fume221215005h

18. S. Abbas, Z. U. Nisa, M. Nazar, M. Amjad, H. Ali, A. Z. Jan, Application of heat and mass transfer to convective flow of Casson fluids in a microchannel with Caputo-Fabrizio derivative approach, *Arab J. Sci. Eng.*, **49** (2024), 1275–1286. https://doi.org/10.1007/s13369-023-08351-1

19. B. S. N. Murthy, M. N. Srinivas, V. Madhusudanan, A. Zeb, E. M. T. Eldin, S. Etemad, et al., The impact of Caputo-Fabrizio fractional derivative and the dynamics of noise on worm propagation in wireless IoT networks, *Alex. Eng. J.*, **91** (2024), 558–579. https://doi.org/10.1016/j.aej.2024.02.027

20. A. Chavada, N. Pathak, Transmission dynamics of breast cancer through Caputo Fabrizio fractional derivative operator with real data, *Math. Model. Control.*, **4** (2024), 119–132. https://doi.org/10.3934/mmc.2024011

21. O. E. Rossler, An equation for hyperchaos, *Physics Lett. A.*, **71** (1979), 155–157. https://doi.org/10.1016/0375-9601(79)90150-6

22. U. Erkan, A. Toktas, Q. Lai, 2D hyperchaotic system based on Schaffer function for image encryption, *Expert Syst. Appl.*, **213** (2023), 119076. https://doi.org/10.1016/j.eswa.2022.119076

23. S. Zhu, X. Deng, W. Zhang, C. Zhu, Construction of a new 2D hyperchaotic map with application in efficient pseudo-random number generator design and color image encryption, *Mathematics.*, **11** (2023), 3171. https://doi.org/10.3390/math11143171

24. J. Tang, Z. Zhang, T. Huang, Two-dimensional cosine-sine interleaved chaotic system for secure communication, *IEEE T. Circuits-II*, **71** (2024), 2479–2483. https://doi.org/10.1109/TCSII.2023.3337145
25. W. Li, W. Yan, R. Zhang, C. Wang, Q. Ding, A new 3D discrete hyperchaotic system and its application in secure transmission, *Int. J. Bifurc. Chaos Appl.*, **29** (2019), 1950206. https://doi.org/10.1142/S0218127419502067
26. W. J. Zhi, C. Z. Qiang, Y. Z. Zhi, The generation of a hyperchaotic system based on a three-dimensional autonomous chaotic system, *Chinese Phys.*, **15** (2006), 6. https://doi.org/10.1088/1009-1963/15/6/015
27. A. Sahasrabuddhe, D. S. Laiphrakpam, Multiple images encryption based on 3D scrambling and hyper-chaotic system, *Inf. Sci.*, **550** (2021), 252–267. https://doi.org/10.1016/j.ins.2020.10.031
28. H. Wang, G. Dong, New dynamics coined in a 4-D quadratic autonomous hyper-chaotic system, *Appl. Math. Comput.*, **346** (2019), 272–286. https://doi.org/10.1016/j.amc.2018.10.006
29. T. Nestor, A. Belazi, B. Abd-El-Atty, M. N. Aslam, C. Volos, N. J. De Dieu, et al., A new 4D hyperchaotic system with dynamics analysis, synchronization, and application to image encryption, *Symmetry*, **14** (2022), 424. https://doi.org/10.3390/sym14020424
30. X. Liu, X. Tong, M. Zhang, Z. Wang, A highly secure image encryption algorithm based on conservative hyperchaotic system and dynamic biogenetic gene algorithms, *Chaos Soliton. Fract.*, **171** (2023), 113450. https://doi.org/10.1016/j.chaos.2023.113450
31. Y. Hui, H. Liu, P. Fang, A DNA image encryption based on a new hyperchaotic system, *Multimed. Tools Appl.*, **82** (2023), 21983–22007. https://doi.org/10.1007/s11042-021-10526-7
32. R. B. Naik, U. Singh, A review on applications of chaotic maps in psuedo-random number generators and encryption, *Ann. Data Sci.*, **11** (2024), 25–50. https://doi.org/10.1007/s40745-021-00364-7
33. T. Bonny, R. A. Debsi, S. Majzoub, A. S. Elwakil, Hardware optimized FPGA implementations of high-speed true random bit generators based on switching-type chaotic oscillators, *Circ. Syst. Signal Pr.*, **38** (2019), 1342–1359. https://doi.org/10.1007/s00034-018-0905-6
34. K. W. Wong, Q. Z. Liu, J. Y. Chen, Simultaneous arithmetic coding and encryption using chaotic maps, *IEEE T. Circuits-II*, **57** (2010), 146–150. https://doi.org/10.1109/TCSII.2010.2040315
35. Z. N. A. Kateeb, S. J. Mohammed, Encrypting an audio file based on integer wavelet transform and hand geometry, *Telkomnika*, **18** (2020). https://doi.org/10.12928/TELKOMNIKA.v18i4.14216
36. K. Benkouider, A. Sambas, T. Bonny, W. A. Nassan, I. A. R. Moghrabi, I. M. Sulaiman, et al., A comprehensive study of the novel 4D hyperchaotic system with self-exited multistability and application in the voice encryption, *Sci. Rep.*, **14** (2024), 12993. https://doi.org/10.1038/s41598-024-63779-1
37. H. Wen, Y. Lin, Z. Xie, T. Liu, Chaos-based block permutation and dynamic sequence multiplexing for video encryption, *Sci. Rep.*, **13** (2023), 14721. https://doi.org/10.1038/s41598-023-41082-9
38. A. Yousefpour, H. Jahanshahi, J. M. M. Pacheco, S. Bekiros, Z. Wei, A fractional-order hyper-chaotic economic system with transient chaos, *Chaos Soliton. Fract.*, **130** (2020), 109400. https://doi.org/10.1016/j.chaos.2019.109400

39. L. Pan, W. Zhou, L. Zhou, K. Sun, Chaos synchronization between two different fractional-order hyperchaotic systems, *Commun. Nonlinear Sci.*, **16** (2011), 2628–2640. https://doi.org/10.1016/j.cnsns.2010.09.016
40. Q. Shi, X. An, L. Xiong, F. Yang, L. Zhang, Dynamic analysis of a fractional-order hyperchaotic system and its application in image encryption, *Phys. Scr.*, **97** (2022), 045201. https://doi.org/10.1088/1402-4896/ac55bb
41. H. Deng, T. Li, Q. Wang, H. Li, A fractional-order hyperchaotic system and its synchronization, *Chaos Soliton. Fract.*, **41** (2009), 962–969. https://doi.org/10.1016/j.chaos.2008.04.034
42. M. A. Balootaki, H. Rahmani, H. Moeinkhah, A. Mohammadzadeh, On the synchronization and stabilization of fractional-order chaotic systems: Recent advances and future perspectives, *Physica A*, **551** (2020), 124203. https://doi.org/10.1016/j.physa.2020.124203
43. Z. A. S. A. Rahman, B. H. Jasim, Y. I. A. Al-Yasir, Y. F. Hu, R. A. A. Alhameed, B. N. Alhasnawi, A new fractional-order chaotic system with its analysis, synchronization, and circuit realization for secure communication applications, *Mathematics*, **9** (2021), 2593. https://doi.org/10.3390/math9202593
44. O. M. Fuentes, J. J. M. Garcia, J. F. G. Aguilar, Generalized synchronization of commensurate fractional-order chaotic systems: Applications in secure information transmission. *Digit. Signal Process.*, **126** (2022), 103494. https://doi.org/10.1016/j.dsp.2022.103494
45. S. Xu, X. Wang, X. Ye, A new fractional-order chaos system of Hopfield neural network and its application in image processing, *Chaos Soliton. Fract.*, **157** (2022), 111889. https://doi.org/10.1016/j.chaos.2022.111889
46. L. Chen, H. Yin, T. Huang, L. Yuan, S. Zheng, L. Yin, Chaos in fractional-order discrete neural networks with application to image encryption, *Neural Networks*, **125** (2020), 174–184. https://doi.org/10.1016/j.neunet.2020.02.008
47. S. Fu, X. F. Cheng, J. Liu, Dynamics, circuit design, feedback control of a new hyperchaotic system and its application in audio encryption, *Sci. Rep.*, **13** (2023), 19385. https://doi.org/10.1038/s41598-023-46161-5
48. J. Losada, J. J. Nieto, Properties of a new fractional derivative without singular kernel, *Progr. Fract. Differ. Appl.*, **1** (2015), 87–92. https://doi.org/10.12785/pfda/010202
49. M. Toufik, A. Atangana, New numerical approximation of fractional derivative with non-local and non-singular kernel, *Eur. Phys. J. Plus.*, **132** (2017), 444. https://doi.org/10.1140/epjp/i2017-11717-0
50. R. Batogna, A. Atangana, New two step Laplace Adam-Bashforth method for integer and noninteger order partial differential equations, *Numer. Meth. Part. D. E.*, **34** (2017), 1739–1785. https://doi.org/10.1002/num.22216

AIMS Press